A LUENBERGER OBSERVER FOR AN INFINITE DIMENSIONAL BILINEAR SYSTEM: A UV DISINFECTION EXAMPLE

D. Vries [*] **K.J. Keesman** [*] **H. Zwart** [**]

[*] *Dept. of Agrotechnology and Food Sciences*
Systems and Control Group
Wageningen University, The Netherlands
[**] *Dept. of Applied Mathematics*
Systems Signals and Control Group
University of Twente, The Netherlands
{*dirk.vries/karel.keesman*}*@wur.nl, h.j.zwart@math.utwente.nl*

Abstract: Inspired by the UV disinfection processes in food and water treatment industry, we design a Luenberger observer which works at the boundary of the infinite dimensional bilinear system. Existence of a solution, stability and some observer design issues are shown. Simulations of a disinfection process and its observer illustrate the results.
Copyright IFAC ©2007

Keywords: bilinear systems, infinite dimensional systems, observers, boundary control, eigenvalue analysis

1. INTRODUCTION

Observers for bilinear infinite dimensional systems with bounded control and observation operator has been studied a decade ago, see Xu et al. (1995); Bounit and Hammouri (1997), and are governed by,

$$\begin{aligned}\dot{\hat{w}}(t) &= A\hat{w}(t) + u(t)B\hat{w}(t) + L(\hat{y}(t) - y(t)) \\ \hat{y}(t) &= C\hat{w}(t), \quad \hat{w}(0) = \hat{w}_0(t) \in H, t \geq 0\end{aligned} \quad (1)$$

where A is an infinitesimal generator of a C_0-semigroup, B and C bounded linear operators, $(w, \hat{w}) \in H$, a real Hilbert space, $(y, \hat{y}) \in Y$ and Y another real Hilbert space. Xu et al. (1995) have shown that for a sufficiently rich input, the observation error converges weakly to zero in the Hilbert space H. Bounit and Hammouri (1997) strengthen the observer results by arriving at sufficient conditions on $(A,\ B,\ C)$ for construction of a strong asymptotic observer. Moreover, in Bounit and Hammouri (2003), a separation principle is deduced for this class of distributed systems.

Interestingly, in many (control) applications where (bio)chemical reactions and transport phenomena occur, measurement and control actions take place at the boundaries. While a theoretical framework already exist (Curtain and Zwart (1995) and references therein), there is ample attention to apply this theory in practice, as far as we know. Note that Bounit and Idrissi (2005) take a different approach by handling the ‘unboundedness’ of the observation and/or control operators based on the notion of ‘admissible’ operators and appropriate regularity assumptions.

In this paper, we analyze a bilinear system where an observer is formulated at the boundary along the lines of Curtain and Zwart (1995). We show some stability and convergence results on the observer. In the upcoming sections, we will not work out the dynamical output feedback problem under bilinear control but instead consider the case with given $u(t)$.

[1] This work is supported by the Technology Foundation STW (grant WWI.6345), applied science division of NWO and the technology programme of the Dutch Ministry of Economic Affairs.

In the example we consider a bilinear distributed parameter system description with one Dirichlet and one Neumann boundary condition. We write the bilinear system into *abstract boundary control* form as follows:

$$\begin{aligned}\dot{z}(t) &= \mathfrak{A}z(t) + B_1 u_1(t) z(t)\\ \mathfrak{B}z(t) &= u_2(t)\\ \mathfrak{C}z(t) &= y(t), \quad z(x,0) = z_0\end{aligned} \tag{2}$$

where $\mathfrak{A} : D(\mathfrak{A}) \subset Z \mapsto Z$ with domain $D(A) = D(\mathfrak{A}) \cap \ker(\mathfrak{B})$ and $Az = \mathfrak{A}z$, for $z \in D(A)$. Furthermore, we have scalar controls $u_i \in U$, $i = \{1, 2\}$, with U a separable Hilbert space. The boundary operators $\mathfrak{B}$ and $\mathfrak{C}$ should be interpreted in the sense of definition 3.3.2 in Curtain and Zwart (1995), where $\mathfrak{B} : D(\mathfrak{B}) \subset Z \mapsto U$ satisfies $D(\mathfrak{A}) \subset D(\mathfrak{B})$ and $\mathfrak{C} : D(\mathfrak{C}) \subset Z \mapsto Y$.

We propose the following Luenberger observer with decreasing error $\epsilon = \hat{z} - z$ as $t \to \infty$,

$$\begin{aligned}\dot{\hat{z}}(t) &= \mathfrak{A}\hat{z}(t) + B_1 u_1(t)\hat{z}(t)\\ \mathfrak{B}^{\text{obs}}\hat{z}(t) &= \begin{pmatrix} u_2(t) \\ L\left(\hat{y}(t) - y(t)\right)\end{pmatrix}\\ \mathfrak{C}^{\text{obs}}\hat{z}(t) &= \hat{y}(t), \quad \hat{z}(x,0) = \hat{z}_0\end{aligned} \tag{3}$$

where the same conditions hold such that (3) is a boundary control system too. Note that, in this case, U is replaced by $\left(U,\ Y\right)^\top$ and u_2 by $\left(u_2,\ (\hat{y} - y)\right)^\top$. In figure 1, a schematic overview is depicted.

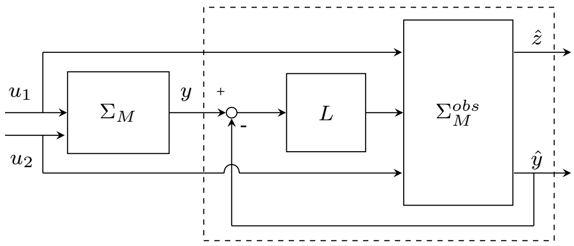

Fig. 1. Schematic overview process (Σ_M)–observer

In the following section, we recall the definition for a boundary control system for a specific example, namely, a UV disinfection process. We show that the differential equation (2) is well posed and show stability properties of an observer as in (3). Furthermore, we will investigate the eigenvalues of the observer–model system. Numerical results are shown in section 4. Finally, section 5 covers some conclusions.

Let us first explore the UV disinfection example.

2. STUDY OF A UV DISINFECTION PROCESS

To have some grip on the matter discussed until now, we study a case where we are inspired by a fluid (water/juice) treatment process where pathogenic biomass is disinfected by UV light. In the sterilization of food, (waste)water treatment and greenhouse technology industries (see some examples in Duse et al. (2003); Guerrero-Beltran and Barbosa-Canovas (2004); Lazarova et al. (1999); Mavrov et al. (1997)), alternative treatment technologies like UV disinfection have gained more attention since they do not leave traces of chemical reagents, such as occurring after chlorination in water treatment processes.

Typically, lamp intensity is *merely* controlled by the turbidity of the to be treated fluid. This is a rather conservative and indirect approach since the actual active pathogenic biomass may differ from the *a priori* assumed amount. In order to efficiently cut lamp energy costs, we would like to implement an observer to use direct biomass measurements for the reconstruction of the pathogen concentration. The disinfection process in an *annular* reactor—mostly used in greenhouse drain water infestation and disinfection of fluid food products—is an interesting case with respect to this aim. Since we want to control the process by the UV lamp and the biomass deactivation is described by first order kinetics, the active biomass state inherits a bilinear relation.

2.1 Modeling assumptions

We take UV treatment in an annular reactor as our model system, with boundary measurements $y(t)$ of the active biomass concentration $z(1,t)$ (by the aid of a 'smart' sensor [2]), as input the fluence rate intensity of the lamp, $u_1(t)$ and a measured boundary disturbance $u_2(t) = z(0,t)$.

More specifically, we assume the following:

(a) in the axial direction, dispersion is modeled by forced plug flow advection plus diffusion. Ideal mixing is assumed in the radial direction.
(b) deactivation of pathogenic organisms is assumed to obey first order reaction kinetics, with constant reaction constant. See Hijnen et al. (2006) and Keesman et al. (2007).
(c) at the end point of the reactor a Neumann boundary is assumed, *i.e.* no dispersion nor inactivation takes place.

Notice that assumption (c) originates from the assumption that the fluid is considered ideally mixed at the outlet (tube) of the reactor and we add to this, that UV irradiation will not penetrate through the reactor walls or reactor outlet.

2.2 UV disinfection process as boundary system

The above assumptions lead to:

$$\begin{aligned}\frac{\partial}{\partial t}z(x,t) =&\alpha\frac{\partial^2}{\partial x^2}z(x,t) - v\frac{\partial}{\partial x}z(x,t)\dots\\ &- \kappa(x)u_1(t)z(x,t), \qquad z(x,0) = z_0(x)\\ z(0,t) =&u_2(t), z(1,t) = y(t), \left.\frac{\partial z}{\partial x}\right|_{(1,t)} = 0\end{aligned} \tag{4}$$

[2] Currently, *on-line* measuring of the metabolic status of cells is still in development, see e.g. Schuster (2000).

where α is the diffusion constant, v the flow velocity and κ a lumped parameter consisting of a susceptibility constant of the micro-organisms w.r.t. the UV-light and the deactivation constant.

We write (4) as an abstract boundary disturbance system (2) where the differential operator is defined as:

$$\mathfrak{A}z = \frac{1}{w}\left(\frac{d}{dx}(p\frac{d}{dx}z)\right) \quad (5)$$

with,

$$p = \alpha e^{-\text{Pe}x}, \quad w(x) = e^{-\text{Pe}x} \quad (6)$$

where $p(x)$, $w(x)$ are real-valued positive continuous functions on $[0, 1]$ with 'Pe' the so-called *Péclet*-number which defines the ratio between convection velocity and diffusion: $\text{Pe} = v/\alpha$. Furthermore, the domain of A is given as,

$$D(A) = \{h \in Z \mid h, \frac{d}{dx}h \text{ absolutely continuous}, \frac{d^2h}{dx^2} \in Z \text{ and } h(0) = 0 = \frac{dh}{dx}(1)\} \quad (7)$$

and the boundary operator,

$$\mathfrak{B}z = z(0, t) = u_2(t) \quad (8)$$

It is straightforward to see that $-A$ is a Sturm-Liouville operator, self-adjoint in a weighted inner product $\langle \cdot, \cdot \rangle_w$ and closed on Z. Furthermore, we define $B_1 = -\kappa(x) = -1_{(x)}$ for $x \in [0, 1]$. In the following we show that (4) permits a mild solution.

2.3 Mild solution

Theorem 1. For (2), where $\mathfrak{A}$ as in (5), there exists a mild solution, with mild solution operator $U(t, s)z_0 = T(t-s)e^{\int_s^t Bu(\tau)d\tau}z_0$, where T is the C_0-semigroup generated by $(A,\ D(A))$.

Proof. The proof originates from the work of Jean Bernoulli on ordinary differential equations. Write $z = vw$, then with $v = T(t-s)v_0$, we get $v\dot{w} = B_1u_1vw$ with z subject to $\dot{z} - Az = B_1u_1z$. It follows that $w = w_0(\exp\int_s^t B_1u_1(\tau)d\tau)$. Substituting $z_0 = v_0w_0$ gives the result. Further, according to Definition 3.2.4 (Curtain and Zwart (1995)), $U(t, s) : \Delta(\tau) \to \mathcal{L}(Z)$ is a mild evolution operator since ($B_1(x)u_1(\tau)$ is replaced by a central dot):

a. $U(s, s) = I$, $s \in [0, \tau]$ holds
b. A generates $T(t)$, which can be written with Riesz bases:

$$T(t, s)z_0 = \sum_{n=1}^{\infty} e^{\mu_n t}\phi_n\langle z_0, \psi_n\rangle$$

Therefore,

$$\begin{aligned} U(t, r)U(r, s) =& T(t-r)e^{\int_r^t \cdot d\tau} \cdot \\ & T(r-s)e^{\int_s^r \cdot d\tau} \\ =& T(t, s)e^{\int_r^t \cdot d\tau + \int_s^t \cdot d\tau} \end{aligned}$$

which equals $U(t, s)$, $0 \le s \le t \le \tau$.
c. It is standard to obtain, $U(\cdot, s)$ is strongly continuous on $[s, \tau]$ and $U(t, \cdot)$ is strongly continuous on $[0, t]$

□

Remark 1. Notice that the above is a general result that apparantly also holds for system (2) if $z = L_2(a, b)$ and $u = L_2(a, b)$.

The aim now is to design an observer for the disinfection process with differential operator $\mathfrak{A}$ as in (5)-(6) and schematically depicted in figure 1.

3. BOUNDARY OBSERVER DESIGN

3.1 System eigenvalue analysis

For the eigenvalues calculation, we apply the separation of variables principle. Therefore, we write $h(x) = c_1e^{\lambda_1 x} + c_2e^{\lambda_2 x}$ and substitute h in $Ah = \mu h$,

For (5)–(6), λ_i becomes

$$\lambda_1(\mu) = \frac{\text{Pe}}{2} + \rho(\mu), \quad \lambda_2(\mu) = \frac{\text{Pe}}{2} - \rho(\mu) \quad (9)$$

with,

$$\rho(\mu) = \sqrt{\frac{\text{Pe}^2}{4} + \frac{\mu}{\alpha}} \quad (10)$$

By using the boundary conditions in $D(A)$, we find $c_1 = -c_2$ and the following relationship between λ_i and μ:

$$\left[\frac{\text{Pe}}{2} + \rho(\mu)\right]e^{\rho(\mu)} - \left[\frac{\text{Pe}}{2} - \rho(\mu)\right]e^{-\rho(\mu)} = 0$$

Since A is self-adjoint in the inner product $\langle \cdot, \cdot \rangle_w$ and negative, $\mu < 0$. Further, we see that $\rho(\mu)$ can only be an imaginary number, $\rho(\mu) = i\omega$, $\omega \in (0, \infty]$. Notice also that μ is always a real number. Thus with Euler's formula we get $i\text{Pe}\sin\omega + i\omega\cos\omega = 0$, hence, we have to find ω at the intersections of

$$\tan\omega = -2\omega/\text{Pe} \quad (11)$$

Consequently, $\rho = \pm i\pi k$ for $k \to \infty$, and for k finite, we have to obtain ω_k numerically. If there is only diffusion ($\text{Pe} = 0$), notice that the eigenvalues indeed reduce to $\mu = -\pi^2k^2$, $k = \{1, \ldots\}$.

3.2 Observer possibilities and eigenvalues

For what will follow, let us first define the weighted inner product:

$$\langle z_1, z_2\rangle_w = \int_0^1 z_1(x)\overline{z_2(x)}w(x)dx \quad (12)$$

with $w(x)$ defined in (6).

Since we measure at $x = 1$ we have two possibilities to design our observer, i.e.,

(i) A Neumann boundary observer, i.e. let (3) be given with $D(A)^{\text{obs}} = D(\mathfrak{A}) \cap \ker(\mathfrak{B}^{\text{obs}})$, as

$$D(A)^{\text{obs}} = \{h \in Z \mid h, \frac{dh}{dx} \text{ absolutely cont.}, \frac{d^2h}{dx^2} \in Z \text{ and } h(0) = 0 = \frac{dh}{dx}(1) - Lh(1)\}$$

and,

$$\mathfrak{B}^{\text{obs}}\hat{z} = \begin{pmatrix} \hat{z}(0,t) \\ \hat{z}(1,t) \end{pmatrix} = L \begin{pmatrix} u_2(t) \\ \hat{y}(t) - y(t) \end{pmatrix}, \quad \mathfrak{C}^{\text{obs}}\hat{z} = \hat{z}(1,t) = \hat{y}(t)$$

(ii) A Dirichlet boundary observer, i.e. let (3) be given with $D(A)^{\text{obs}} = D(\mathfrak{A}) \cap \ker(\mathfrak{B}^{\text{obs}})$ as in the Neumann boundary observer (i), except that the boundary conditions in $D(A)^{\text{obs}}$ are replaced by $h(0) = 0 = h(1) - Lh(1)$. Furthermore, $\mathfrak{B}^{\text{obs}}$ and $\mathfrak{C}^{\text{obs}}$ are as in the Neumann boundary observer (i).

Let us inspect the eigenvalues of the error dynamics, i.e. $\mathfrak{A}\epsilon = \mu_k\epsilon$ for both observer possibilities (i) and (ii). Possibility (ii) leads to a Luenberger gain $L = 1$, independent of the outcome for μ. As a consequence, in order to have control on our error dynamics, our choice reduces to the Neumann boundary observer (i).

Again, we get for (5)–(6), λ_i as in (9). With the boundary conditions of $D(A^{\text{obs}})$ we get the following relation between $\rho(\mu)$ (10) and the observer gain L,

$$\Big[\frac{\text{Pe}}{2} + \rho - L\Big]e^{\rho} - \Big[\frac{\text{Pe}}{2} - \rho - L\Big]e^{-\rho} = 0$$

A^{obs} is self-adjoint in the inner product $\langle \cdot, \cdot \rangle_w$. We check if it is negative.

Theorem 2. (Negativity of operator). $\mathfrak{A}$ in (5)–(6) generates a C_0-semigroup and for $u \in \mathbb{R}^+$, the operator A^{obs} is negative $\forall z_0 \in Z$, $L < 0$. The error $\epsilon = \hat{z} - z \to 0$ as $t \to \infty$.

Proof. It is sufficient to check the time derivative of the norm of the observer error, $\frac{d}{dt}\sqrt{\|\epsilon\|} = \langle \epsilon, \mathfrak{A}\epsilon + B_1u_1\epsilon\rangle \leq 0$ using the inner product (12). It follows that

$$\begin{aligned}\frac{d}{dt}\epsilon(x,t) = 2\Big[&\epsilon(x,t)p(x)\frac{\partial \epsilon(x,t)}{\partial x}\Big|_{x=0}^{x=1} \dots \\ &- \int_0^1 p(x)\frac{\partial}{\partial x}\epsilon(x,t)^2 dx \dots \\ &+ \int_0^1 w(x)B(x)u_1(t)\epsilon(x,t)^2 dx\Big]\end{aligned}$$

Assume now $u_1 \equiv 0$. It follows that the first right term is smaller than zero for all $L \in [-\infty, 0)$, hence A^{obs} is negative. The second and third right term are both smaller than zero since $B(x)u_1(t) < 0$ and $p(x) > 0$. $\square$

Since for $L \leq 0$, A^{obs} is negative and thus $\mu < 0$. Again, $\rho = i\omega$, $\omega \in (0, \infty]$ and $\mu \in \mathbb{R}^-$. With the aid of Euler's formula we get,

$$\tan\omega = \frac{\omega}{L - \text{Pe}/2} \tag{13}$$

where the intersections ω_k with $k = \{0, 1, \dots, \infty\}$ of (13) can be calculated numerically. We can already deduce from (13) or figure 2, that

- for fixed k,
$$\lim_{L \to -\infty} \omega_k = k\pi$$
- for fixed $L \in [-\infty, 0)$,
$$\omega_k \in \big[(k - \frac{1}{2})\pi, k\pi\big], \quad \Leftrightarrow \quad \lim_{k\to\infty} \frac{\omega_k}{(k-\frac{1}{2})\pi} = 1$$

3.3 Mild solution in Riesz bases

The mild solution of (4) with or without the Neumann boundary observer can be directly written in orthogonal Riesz bases. By Theorem 1 and given that $B_1 = -1_{(x)}$,

$$\begin{aligned} z(\cdot, t) &= U(t,0)z_0(\cdot,t) \\ &= \sum_{k=1}^{\infty} e^{\mu_k t}\phi_k\langle z_0, \phi_k\rangle e^{-\int_0^t 1_{(\cdot)}u_1(t)d\tau}\end{aligned}$$

with μ_k the (numerical) solutions of (11) and (13), respectively, and associated eigenvectors $\phi_k = \sin\rho(\mu_k)x$, where $\rho(\mu_k)$ is given by (10).

3.4 More on eigenvalues: the LTI/LTV case

Suppose we have a constant lamp strength, let $u_1 = 1$. Then, the eigenvalues of the system and the observer are directly influenced by the magnitude of $B_1(x) = -\kappa(x)$. If we assume furthermore that κ is space invariant, then $\tilde{\rho}(\tilde{\mu})$ in (10) is now given as,

$$\tilde{\rho}(\mu) = \sqrt{\frac{\text{Pe}^2}{4} + \frac{\tilde{\mu} + \kappa}{\alpha}}$$

which clearly effects $\tilde{\mu}$, since now

$$\tilde{\mu}_k = \alpha\left(-\omega_k^2 - \text{Pe}^2/4 - \kappa\right)$$

and equation (13) still applies (for the system without observer, set $L = 0$). In the time-variant case, we specify a known input signal $s(t) \triangleq u_1(t) \in [0, s_{\max}]$. The eigenvalues will then vary between,

$$-\omega_k^2 - \frac{\text{Pe}^2}{4} - \kappa s_{\max} < \frac{\tilde{\mu}_k}{\alpha} < -\omega_k^2 - \frac{\text{Pe}^2}{4}$$

3.5 What is the performance increase if we change L?

From the above it follows that for $L < 0$, $k \neq 0$ (since A^{obs} is negative), the *growth bound* (maximal eigenvalue) becomes $\mu_\circ/\alpha = \text{Pe}^2/4 - \omega_\circ^2$ with $\pi/2 < \omega_\circ < \pi$. For decreasing L, the system becomes more stable, but not spectacular since the nominal ($L = 0$) frequency $\omega_\circ$ can be shifted by at most $\pi/2$ for some L and fixed k. Consequently, we can also say something about the maximal performance increase if we push the eigenvalues by L. Let the (performance) margin be defined as the difference between the nominal growth bound and the new growth bound μ^*, i.e. $\Delta_\mu := \mu_\circ - \mu^*$. Let the shift in the smallest frequency be defined as $\Delta_\omega := \omega_\circ - \omega_*$. Then, by rewriting $\rho = i\omega$ in $\mu(\rho)$ we get,

$$\begin{aligned} \Delta_\mu &= \mu_\circ - \mu^* \Leftrightarrow^{\text{substitute } \rho \text{ in (10)}} \\ &= \omega_*^2 - \omega_\circ^2 \Leftrightarrow^{\text{substitute } \omega_* = \omega_\circ - \Delta_\omega} \\ &= -2\Delta_\omega\omega_\circ + \Delta_\omega^2 \end{aligned}$$

Since $\pi/2 < \omega_\circ < \pi$ and $0 < \Delta_\omega < \pi/2$, it follows that $0 < \Delta_\mu < \frac{3}{4}\pi^2$.

4. NUMERICAL RESULTS

4.1 Numerical eigenvalue and observer gain analysis

With the aid of a Nelder-Mead direct search method, ω_k for $k = \{1, 2\}$ at the intersections of (13) are found by solving

$$\min_{\omega_k \in [(k-\frac{1}{2})\pi, k\pi]} \left|\tan\omega_k - \omega_k/(L - \mathrm{Pe}/2)\right|$$

from which $\mu_\circ$ is obtained for some fixed L and Pe-number. Figure 2 gives us a first impression where these intersections will be for different values of L and fixed Pe $= 1/2$. Figure 3 and 4 show the behavior of

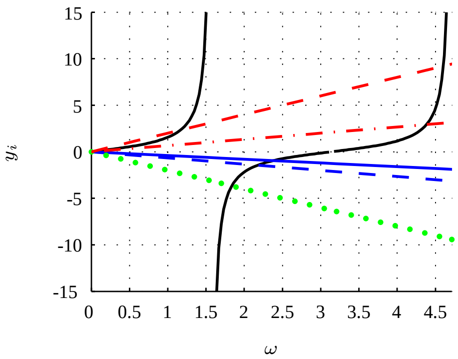

Fig. 2. Graph of $y_1 = \tan\omega$ [–] and $y_2 = \omega/(L - \frac{1}{4})$ vs. ω for $L = -2$ [–], $L = -1$ [– –], $L = 0$ [•], $L = 1$ [– –] and $L = 2$ [– ·]

the growth bound for Pe $\in [0, 5]$ and $L \in [-20, 5]$ with equidistant spacing such that singularities at $2L = $ Pe do not occur. Indeed, the larger Pe-numbers, the larger the growth bound and the lesser the effect of the observer gain. Notice also that for $L > 0$, the growth bound tends to zero and the observer–system becomes less stable.

To find out the size of L for a given performance *increase* Δ_μ, we have calculated L^* for which *Péclet*-numbers the performance measure is obtained. The results are depicted in figure 5, where $-L$ is shown for reasons of eligibility. We see that for increasing Pe, $-L^*$ increases rapidly.

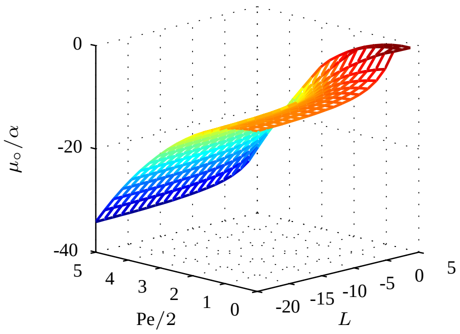

Fig. 3. Growth bound ($\mu_\circ$) vs. Pe and L

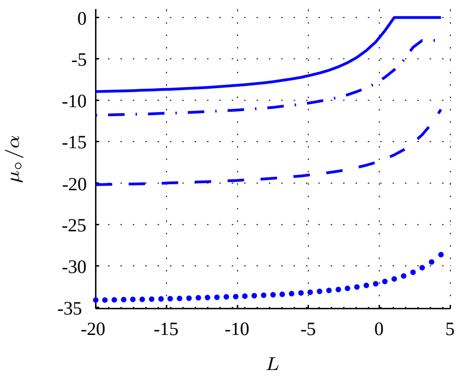

Fig. 4. Growth bound vs. L with fixed Pe, i.e. for Pe$/2 = 0$ [–], 1.67 [– ·], 3.33 [– –] and 5 [•]

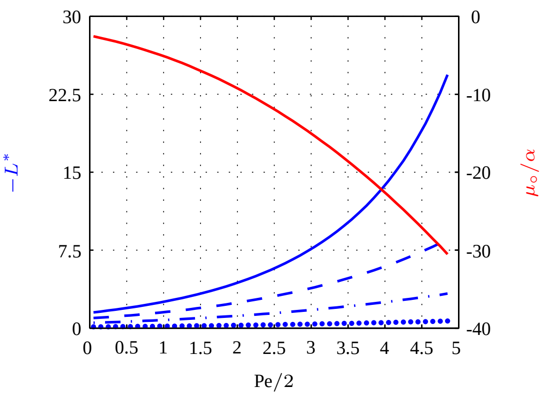

Fig. 5. Left y-axis (blue): calculated L^* for different growth margins Δ_μ, i.e. for $\Delta_\mu = 0.25$ [•], 0.92 [– ·], 1.58 [– –] and 2.25 [–]. Right y -axis (red), i.e. calculated $\mu_\circ$ [–] ($L^* = 0$) vs. Pe.

4.2 Finite difference simulation

To check whether the above analysis is a good indication for practical simulation and/or experiments, we simulate the system with the aid of centralized finite differences and a stiff ODE solver (`ode15s`). We simulate the time variant case, i.e. the input u_1 is known and is generated as a positive oscillating signal around 1: $u_1(t) = 1 + (\cos 4\pi t)/2$. Further, we let the boundary disturbance u_2 oscillate too: $u_2(t) = \sin^2 3\pi t$. Parameters are set as $\alpha = 1$, $v = .1$, $\kappa = -1$, $z_0 = 0$ and a spatial grid of 81 points. Furthermore we start the simulation with a wrong estimate of z_0, that is, we let it believe to be $\hat{z}_0 = 0.3$. The state variable z and output (at $x = 1$) are depicted in figure 6. Figure 7 clearly shows that the error converges rapidly to zero for $L = -5$, faster than the 'no–observer' case (for eligibility, $t \in [0, 4]$).

The smallest eigenvalue of the process without inactivation is $\mu_\circ^{\text{fd}} = -2.51$ (fd stands for finite difference system). The eigenvalue of the observer LTV system is estimated as $\tilde{\mu}_*^{\text{fd}} \approx -3.51$ (we assume $B_1 u_1 \approx -1$). For the process we calculate $\mu_\circ^{\text{fd}} = -2.51$ which corresponds to $\omega_\circ^{\text{fd}} = 1.58$, and comes indeed close to the solution of (13): $\omega_\circ = 1.632$. With observer, where $L = -5$, we get an almost identical result: $\mu_*^{\text{fd}} = -6.91$ cf. $\mu_* = -7.089$.

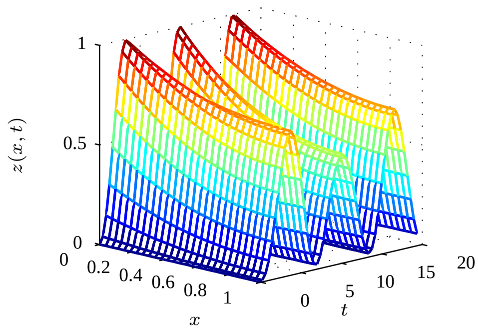

Fig. 6. State $z(x, t)$ (biomass concentration)

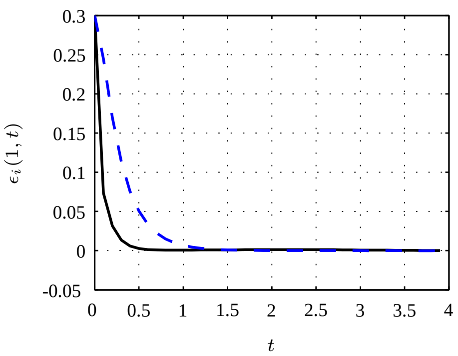

Fig. 7. Error responses, where $\epsilon_1(t) \triangleq \hat{y}(t) - y_m(t)$ [–] and $\epsilon_2(t) := z(1, t) - y_m(t)$ [- -]

5. CONCLUSIONS

Inspired by a UV disinfection processes in food and water treatment industry, we designed a Luenberger observer which works at the boundary of the infinite dimensional bilinear system. We worked out the example in a *boundary control* setting and gave results on the solution and stability, and extensively explored eigenvalues of the system.

From the analysis it follows that for mild Péclet-numbers (Pe $\ll 1$, hence a low convection–diffusion ratio), there is more room to obtain a performance gain with a suitable observer gain L. For large Péclet numbers, fast process dynamics already push the estimation error to zero. In this case one may decide to choose a small positive (destabilizing) L to smooth the error.

Furthermore, analyzing the system in the infinite dimensional setting gives a good impression how the system will behave, *independent* of some choice of discretization or other finite approximation method.

Note that in this paper, we have not provided controllability and observability results due to lack of space. However, we can state that our example is not controllable, but is detectable and approximately observable. Moreover, if we assume some smoothness on $u_2(t)$ and $\epsilon(t)$ and rewrite our example into an extended state space system to arrive at (1), the separation principle (Bounit and Hammouri (2003)) may certainly be applied.

REFERENCES

H. Bounit and H. Hammouri. A separation principle for distributed dissipative bilinear systems. *IEEE T. Automat. Contr.*, 48(3):479–483, 2003.

H. Bounit and H. Hammouri. Observers for infinite dimensional bilinear systems. *Eur. J. Control*, 3(1): 325–339, 1997.

H. Bounit and A. Idrissi. Regular bilinear systems. *IMA J. Math. Control Inf.*, 22(1):26–57, 2005.

R.F. Curtain and H. Zwart. *An Introduction to Infinite Dimensional Linear Systems Theory*. Springer-Verlag, New York, 1995.

A. G. Duse, M. P. da Silva, and I. Zietsman. Coping with hygiene in south africa, a water scarce country. *Int. J. Environ. Heal. R.*, 13:S95–S105, 2003.

J. A. Guerrero-Beltran and G. V. Barbosa-Canovas. Review: Advantages and limitations on processing foods by uv light. *Food Sci. Technol. Int.*, 10(3): 137–147, 2004.

W. A. M. Hijnen, E. F. Beerendonk, and G. J. Medema. Inactivation credit of uv radiation for viruses, bacteria and protozoan (oo)cysts in water: A review. *Water Res.*, 40(1):3–22, 2006.

K.J. Keesman, D. Vries, S. van Mourik, and H. Zwart. Modeling and control of water disinfection process in annular photoreactors. *Accepted for ECC'07*, 2007.

V. Lazarova, P. Savoye, M. L. Janex, E. R. Blatchley, and M. Pommepuy. Advanced wastewater disinfection technologies: State of the art and perspectives. *Water Sci. Technol.*, 40(4-5):203–213, 1999.

V. Mavrov, A. Fahnrich, and H. Chmiel. Treatment of low-contaminated waste water from the food industry to produce water of drinking quality for reuse. *Desalination*, 113(2-3):197–203, 1997.

K.C. Schuster. Monitoring the physiological status in bioprocesses on the cellular level. *Adv. Biochem. Eng. Biot.*, Volume 66:185–208, 2000.

C. Z. Xu, P. Ligarius, and J. P. Gauthier. An observer for infinite-dimensional dissipative bilinear-systems. *Comput. Math. Appl.*, 29(7):13–21, 1995.